Proceedings of the 2013 International Symposium on Liquid Metal Processing & Casting
Edited by: Matthew J. M. Krane, Alain Jardy, Rodney L. Williamson, and Joseph J. Beaman
TMS (The Minerals, Metals & Materials Society), 2013

THERMODYNAMICS FOR THE INFLUENCE OF SLAG COMPOSITION ON THE INCLUSION CONTROL IN SEMI-KILLED LIQUID STEELS

Joo Hyun Park[1,*], Jun Seok Park[1]
[1]Department of Materials Engineering, Hanyang University, Ansan 426-791, Korea
* contact email ; basicity@hanyang.ac.kr

Keywords: CaO-Al_2O_3-SiO_2-CaF_2-MgO(-MnO) slag, Si-Mn-killed steel, Inclusion, Slag basicity, Slag-Steel-Inclusion multiphase equilibria, Alumina ladle

Abstract

Thermodynamic equilibria between CaO-Al_2O_3-SiO_2-CaF_2-MgO (-MnO) slag and Fe-1.5%Mn-0.5%Si-0.5%Cr steel was investigated at 1873 K to understand the effect of slag composition on the concentration of Al_2O_3 in the inclusions in Si-Mn-killed steels. The composition of the inclusions were mainly equal to $(MnO)/(SiO_2)$=0.8(±0.06) (mole ratio) with various Al_2O_3 content which increased by increasing the basicity of slag. The concentration ratio of the inclusion components, $(MnO \times Al_2O_3/SiO_2)$ and the activity ratio of the steel components showed a good linear relationship in a logarithmic scale, indicating that the activity coefficient ratio of the inclusion components was not significantly changed. From the slag-metal-inclusion multiphase equilibria, the concentration of Al_2O_3 in the inclusions was expressed as a linear function of the activity ratio of the slag components in a logarithmic scale. Consequently, the compositional window of the slag for obtaining the inclusions with low melting point in the Si-Mn-killed steel treated in an alumina refractory was recommended.

Introduction

Non-metallic inclusions in steel cause deterioration of mechanical properties as well as severe problems during steel processing.[1-3] The cleanliness of the steel is important in spring steel and tire cord steel since nonmetallic inclusions act as crack initiation sites when subjected to cyclic stress. However, no steel can be totally free from inclusions. For this reason, Si and Mn are generally used as deoxidizers in spring steel and tire cord steel in order to avoid harmful Al_2O_3-rich inclusions.[4,5] A number of studies have been carried out to identify techniques that achieve inclusions that are as harmless as possible.[4-18] The application of optimized slag to suppress the formation of harmful inclusions such as alumina and spinel is one such method used for various steel grades including Si-Mn-killed steel.

For these reasons, the MnO-Al_2O_3-SiO_2 ternary system has gained attention for several decades. Many studies have been performed to fundamentally understand this oxide system in terms of thermodynamics.[6-10] Thanks to previous work, if we determine the concentration range of Mn, Si, Al, and O in molten steel, we can predict the corresponding composition window for MnO, SiO_2 and Al_2O_3 in the above inclusion system. Based on this background, several researchers suggested deoxidation for liquid inclusion in the MnO-Al_2O_3-SiO_2 system.

Kang and Lee reported that inclusions having a MnO/SiO_2 mass% ratio near unity and Al_2O_3 content in the range of 10~20 mass% have low liquidus temperatures (~1473 K) and suggested that a Mn/Si ratio of 2~5 meets these conditions when Mn+Si=1.0% in the steel.[9] Bertrand et al.[12] found that slag composition during secondary metallurgy must have a low basicity (CaO/SiO_2), and Al content in the steel should be maintained under 15 ppm to avoid the formation of Al_2O_3. Chen et al.[5] studied the effect of top slag on the inclusion composition in tire cord steel and found that inclusion plasticization can be achieved by controlling the binary basicity of top slag (CaO/SiO_2) around 1.0 and maintaining the Al_2O_3 content in top slag below 10%. However, an experimental study to identify conditions for obtaining liquid inclusion when the slag has relatively high basicity (CaO/SiO_2) coupled with Al_2O_3 saturation, which corresponds to the alumina refractory lining, has not yet been conducted.

Therefore, in the present study, the equilibria between CaO-Al_2O_3-SiO_2-CaF_2-MgO(-MnO) slag and Fe-1.5%Mn-0.5%Si-0.5%Cr melt was investigated at 1873 K in order to understand the effect of slag composition on the concentration of Al_2O_3 in the inclusions.

Experimental

A Fe-1.5%Mn-0.5%Si-0.5%Cr alloy (235 g), Fe-0.23(±0.02)%O alloy (65 g) and CaO-Al_2O_3-SiO_2-CaF_2-MgO(-MnO) slag (CaO/SiO_2=0.5~2.0) were equilibrated for an hour at 1873 K in a fused alumina crucible (60 mm × 52 mm × 120 mm) with a graphite heater under an Ar-3%H_2 gas atmosphere using an induction furnace. The Fe-0.23(±0.02)%O alloy was prepared in an MgO crucible by blowing oxygen gas on Fe melt for 20 minutes using an induction furnace. The slags were pre-melted in a graphite crucible for two hours in an electric resistance furnace. Some slags, disintegrated into fine powders due to high basicity, were pelletized to enable accurate addition to the melt surface.

Temperature was controlled by a B-type thermocouple. After the temperature reached 1903 K, Fe-O alloy was added to the Fe-Si-Mn-Cr melt under an inert atmosphere to control the initial oxygen content. The slag was then added to the melt when the temperature was recovered to 1873 K. After a period of 60 minutes, which was preliminarily determined to achieve equilibrium, sampling was performed using a quartz tube and then the samples were directly quenched by dipping them in brine.

The chemical composition of each steel sample was determined by ICP-AES, and the nitrogen and oxygen content was analyzed using a combustion analyzer. The characteristics of inclusions including 3-dimensional morphology and chemical composition were analyzed using the potentiostatic electrolytic extraction method and SEM-EDS. Details regarding characterization of inclusions are given in previously published articles.[19,20] The

composition of the inclusion in each sample was taken as the average of about ten inclusions.

Results and Discussion

The following reactions occurred at the slag-metal interface:[21,22]

$$2[Al] + 3[O] = (Al_2O_3)^{slag} \quad [1]$$

$$\log K_{[1]} = \log\left[\frac{a^s_{Al_2O_3}}{a^2_{Al} \cdot a^3_O}\right] = 13.60 \quad (\text{at } 1873\,K) \quad [2]$$

$$[Si] + 2[O] = (SiO_2)^{slag} \quad [3]$$

$$\log K_{[3]} = \log\left[\frac{a^s_{SiO_2}}{a_{Si} \cdot a^2_O}\right] = 4.67 \quad (\text{at } 1873\,K) \quad [4]$$

where $K_{[n]}$ and a_i are the equilibrium constant of Eq. [n] and the activity of element i in molten steel. The superscript s represents the 'slag' phase. The activity of oxygen determined by the equilibrium of $[Al]/(Al_2O_3)$, a_O^{Al} and by $[Si]/(SiO_2)$, a_O^{Si} can be estimated from Eqs. [5] and [6], respectively.

$$\log a_O^{Al} = \frac{1}{3}(\log a^s_{Al_2O_3} - 2\log a_{Al} - \log K_{[1]}) \quad [5]$$

$$\log a_O^{Si} = \frac{1}{2}(\log a^s_{SiO_2} - \log a_{Si} - \log K_{[3]}) \quad [6]$$

In addition, the activity coefficient of solute element (M) can be calculated by classical Wagner formalism using the first- and second-order interaction parameters, which are listed in Table I.[21-28]

$$\log f_M = \sum_{i=Cr,\,Si,\,Mn,\,Al,\,O} (e^i_M \times [\%i] + r^i_M \times [\%i]^2) \quad [7]$$

where f_M, e^i_M and r^i_M are the Henrian activity coefficient of element M, and the first- and second-order interaction parameters between M and i, respectively.

Table I. Interaction Parameters Used in the Present Study.[21]

e_i^j (r_i^j)	Cr	Si	Mn	Al	O
Al	0.03[27]	0.056	0.035[28]	0.043	-1.98 (39.8)[26]
Si	-0.021[23]	0.1	-0.007[17]	0.058	-0.12
O	-0.032[24]	-0.066	-0.037[25]	-1.17 (-0.01)[26]	-0.17

The activities of oxygen calculated from the $[Al]/(Al_2O_3)$ and $[Si]/(SiO_2)$ equilibria are plotted against the activity of oxygen determined from classical Wagner formalism as shown in Figure 1. The activity of Al_2O_3 and SiO_2 in the slag at 1873 K was also calculated using thermodynamic software, FactSage™6.3, assuming that the CaF_2 (~10%) does not seriously affect the activity of slag components. This software has been successfully applied to compute the phase equilibria of multicomponent steel and oxide systems.[15-20,29-47]

The activities of oxygen calculated from the $[Si]/(SiO_2)$ and $[Al]/(Al_2O_3)$ equilibria were in good agreement with that from classical Wagner formalism, while several points for the activity of oxygen calculated from the $[Al]/(Al_2O_3)$ equilibrium were slightly higher than those determined using Wagner formalism. This scatter is probably due to the fact that the concentration of total Al, instead of dissolved Al, was used when the activity of Al in molten steel was calculated.[48] Nevertheless, the slag-metal reaction is believed to have been in equilibrium in the present experiments.

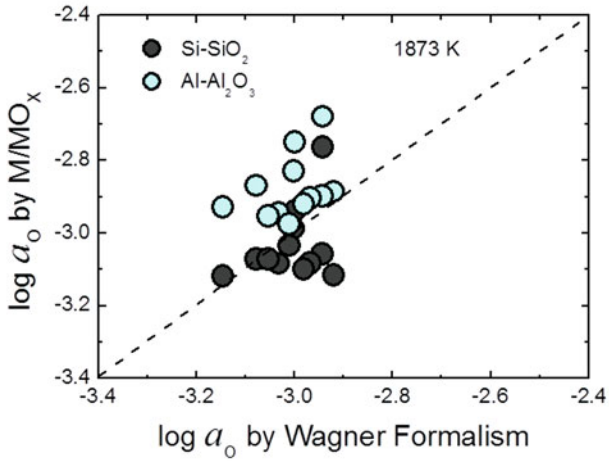

Fig. 1. Relationship between activities of oxygen calculated from classical Wagner formalism and deoxidation equilibria by aluminum and silicon.

The composition of the inclusions is plotted on the MnO-Al_2O_3-SiO_2 ternary phase diagram as shown in Figure 2, which was generated by FactSage™6.3 with the FToxid database at 1873 K and $p(O_2)=10^{-10}$ atm. Five solid phases, SiO_2, MnO, $MnAl_2O_4$, Al_2O_3 and $Al_6Si_2O_{13}$ (mullite), are shown to be in equilibrium with the liquid phase. All of the inclusions were located in the liquid phase and their compositions were nearly equal to $(MnO)/(SiO_2)=0.8(\pm 0.06)$ in mole ratio. The only exception was sample #1, the composition of which corresponded to high silica area because of the relatively low aluminum content in molten steel in conjunction with the high activity of SiO_2 in slag.

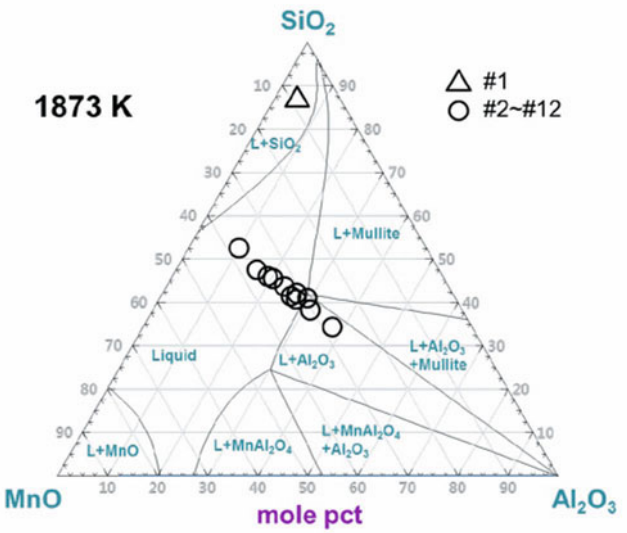

Fig. 2. Computed phase diagram of the MnO-Al_2O_3-SiO_2 system at 1873 K and $p(O_2)=10^{-10}$ atm. The triangles and circles are the average composition of ten inclusions per sample.

The effect of slag basicity (=CaO/SiO_2 ratio) on the concentration of alumina in the inclusions at 1873 K is shown in Figure 3. The alumina content in the inclusions increased with increasing slag basicity up to about C/S=1.5, followed by some variation in the Al_2O_3 content around 40(±10)% when the C/S ratio was greater than 1.5. When the basicity of the slag was greater than 1.5 (#4~#12), the slag was saturated by Al_2O_3-rich phase such as $CaO•2Al_2O_3$ or $CaO•6Al_2O_3$, whereas the alumina content was dependent on the slag basicity when the basicity was lower than 1.5 (#1~#3). Hence, the content of alumina in the inclusions is strongly affected by the activity of alumina in the slag in equilibrium with molten steel.

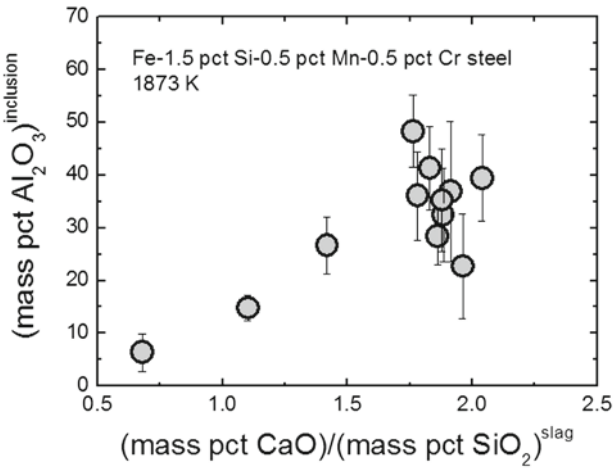

Fig. 3. Effect of the ratio of CaO/SiO_2 in the slag on the concentration of Al_2O_3 in the inclusions.

The effect of alumina content on the melting point and the primary crystalline phase of the inclusion is shown in Figure 4. The liquidus surface of the $(MnO)/(SiO_2)$=1.0 join in the MnO-SiO_2-Al_2O_3 inclusion system at 1873 K was calculated using the FactSage™6.3 program. Increasing the concentration of alumina in the inclusions changed the primary phase in the order of $MnSiO_3$ (rhodonite), $Mn_3Al_2Si_3O_{12}$ (spessartite), $MnAl_2O_4$ (galaxite) and Al_2O_3. The melting point of the inclusion decreased with increasing alumina concentration up to about 8%, followed by a rebound after this composition.

When the slag basicity was relatively low, i.e. C/S < 1.5, the melting point of the inclusion was lower than 1623 K and the primary crystalline phases were spessartite and galaxite. In contrast, the melting point of inclusions ranged from about 1523 to 2023 K and the crystalline phase was mainly alumina when the basicity of the slag was greater than 1.5. Therefore, controlling the slag basicity to be less than 1.5 is recommended in order to avoid Al_2O_3-rich inclusions during both the refining stage and the solidification process.

The oxide-forming elements including Al, Si and Mn in molten steel are in equilibrium with not only the slag phase as shown in Eqs. [1] and [3], but also the inclusion phase as indicated in Eqs. [8], [10] and [12].

$$2[Al] + 3[O] = (Al_2O_3)^{inclusion} \quad [8]$$

$$\log K_{[8]} = \log X^i_{Al_2O_3} + \log \gamma^i_{Al_2O_3} - 2\log a_{Al} - 3\log a_O \quad [9]$$

$$[Si] + 2[O] = (SiO_2)^{inclusion} \quad [10]$$

$$\log K_{[10]} = \log X^i_{SiO_2} + \log \gamma^i_{SiO_2} - \log a_{Si} - 2\log a_O \quad [11]$$

$$[Mn] + [O] = (MnO)^{inclusion} \quad [12]$$

$$\log K_{[12]} = \log X^i_{MnO} + \log \gamma^i_{MnO} - \log a_{Mn} - \log a_O \quad [13]$$

where the superscript *i* represents the 'inclusion' phase. By combining Eqs. [9], [11] and [13], the following equation can be deduced:

$$\log\left(\frac{X^i_{Al_2O_3}\cdot X^i_{MnO}}{X^i_{SiO_2}}\right) = \log\left[\frac{a^2_{Al}\cdot a_{Mn}\cdot a^2_O}{a_{Si}}\right] + \log\left(\frac{\gamma^i_{SiO_2}}{\gamma^i_{Al_2O_3}\cdot\gamma^i_{MnO}}\right) + C \quad [14]$$

where *C* is constant at a given temperature. From Eq. [14], the molar composition ratio of the inclusions, viz. $MnO\times Al_2O_3$ to SiO_2 will be directly proportional to the activity ratio of steel composition ($Al^2\times Mn\times O^2$ to Si) on a logarithmic scale if the activity coefficient ratio of the inclusions would not be seriously changed. In order to calculate the activity of steel components, the activity coefficient of each element was calculated using Eq. [7], and the interaction parameters listed in Table I.

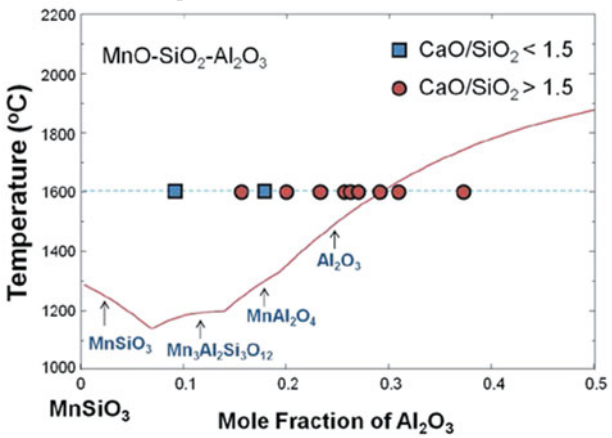

Fig. 4. Calculated liquidus temperatures in the MnO-SiO_2-Al_2O_3 systems as a function of the concentration of Al_2O_3 when the ratio of MnO to SiO_2 (mol%) is unity.

The relationship between $\log(X_{Al_2O_3}\cdot X_{MnO}/X_{SiO_2})$ and $\log[a^2_{Al}\cdot a_{Mn}\cdot a^2_O/a_{Si}]$ is shown in Figure 5. A linear correlation between them is evident with a slope of 1.2 within experimental scatters, which is relatively close to unity within the composition range investigated in the present study. Therefore, it is concluded that the components in molten steel and each oxide in the inclusions are in equilibrium and that the activity coefficient ratio of oxide components in the inclusions (second term on the right-hand side in Eq. [14]) would be constant under the present experimental conditions.

Alternatively, the activities of the components in molten steel are also affected by those of their oxide components in the slag phase as indicated by Eqs. [1], [3] and [15].[21]

$$[Mn] + [O] = (MnO)^{slag} \qquad [15]$$

$$\log K_{[15]} = \log\left[\frac{a^s_{MnO}}{a_{Mn} \cdot a_O}\right] = 1.27 \quad (\text{at } 1873\,\text{K}) \qquad [16]$$

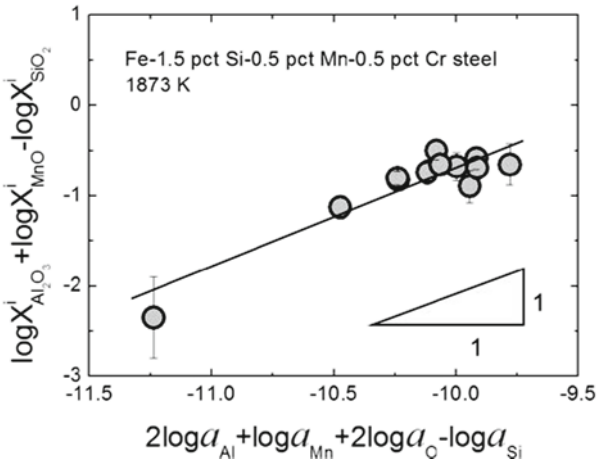

Fig. 5. Effect of activities of Al, Mn, Si and O on composition of inclusions in steel at 1873 K.

By combining Eqs. [2], [4], [14] and [16], the following equation can be deduced:

$$\log X^i_{Al_2O_3} + \log\left(\frac{X^i_{MnO}}{X^i_{SiO_2}}\right) = \log\left(\frac{a^s_{Al_2O_3} \cdot a^s_{MnO}}{a^s_{SiO_2}}\right) + \log\left(\frac{\gamma^i_{SiO_2}}{\gamma^i_{Al_2O_3} \cdot \gamma^i_{MnO}}\right) + C \qquad [17]$$

This equation implies that the activity ratio of slag components directly affects the concentration of the inclusions since the activity coefficient ratio of the inclusion components can be assumed to be constant from Figure 5 and Eq. [14]. Furthermore, Figure 2 (excluding sample #1) indicates that the molar concentration ratio of MnO to SiO_2 in the inclusions is constant, i.e., 0.8(±0.06). Consequently, Eq. [17] can be simplified to Eq. [18].

$$\log X^i_{Al_2O_3} = \log\left(\frac{a^s_{Al_2O_3} \cdot a^s_{MnO}}{a^s_{SiO_2}}\right) + C' \qquad [18]$$

Thus, it is simply expected that there is a linear relationship between $\log X^i_{Al_2O_3}$ and $\log(a^s_{Al_2O_3} \cdot a^s_{MnO} / a^s_{SiO_2})$ with a slope of unity, which is confirmed by the result shown in Figure 6. The slope of the line was found to be 1.1 from linear regression analysis. Even though there were some experimental scatters, this result qualitatively implies that the activity ratio of slag components directly affects the concentration of alumina in the inclusions.

Actually, from the FactSage™6.3 computation, the activity of Al_2O_3 and MnO in the slags investigated in the present study was found to range from about 0.5 to 0.9 and from 0.015 to 0.03 (approximately two-fold increase), respectively. However, the activity of SiO_2 varied from about 0.01 to 0.1, i.e. a ten-fold increase within the present composition range. The iso-activity contours of Al_2O_3, MnO, and SiO_2 in the CaO-SiO_2-Al_2O_3-5% MnO slag system at 1873 K are shown in Figure 7.

The results shown in Figure 4 indicate that the Al_2O_3 content in the inclusions should be kept lower than about 18% in order to maintain the melting point of the inclusions below 1573 K. Hence, from Figure 6, the activity ratio of the slag components, $(a^s_{Al_2O_3} \cdot a^s_{MnO} / a^s_{SiO_2})$, should be lower than unity.

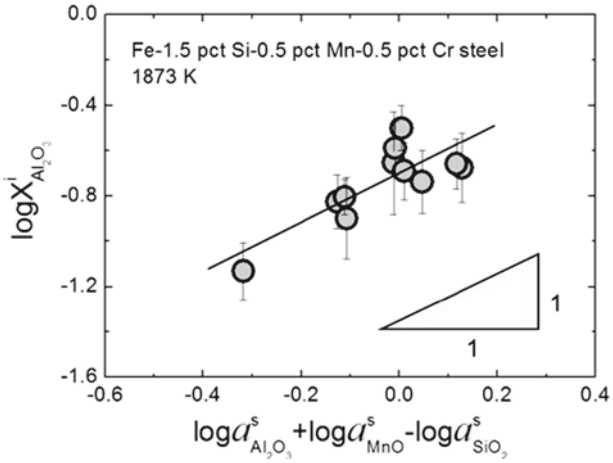

Fig. 6. Effect of activities of Al_2O_3, MnO and SiO_2 in the slag on the concentration of Al_2O_3 in the inclusion.

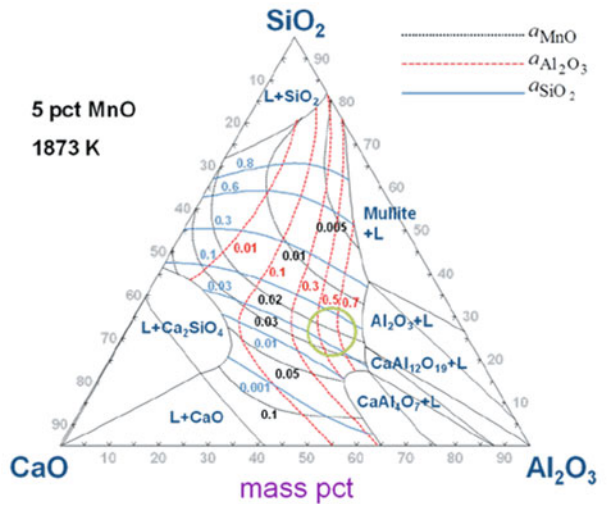

Fig. 7. Iso-activity contours of MnO, Al_2O_3 and SiO_2 in the CaO-SiO_2-Al_2O_3-5%MnO slag at 1873 K. The circle is the recommended slag composition for obtaining liquid inclusion of which melting point is lower than 1573 K in Si-Mn-killed steel refined in the alumina ladle.

Because the activity of Al_2O_3 in the slags ranged from about 0.5 to 0.9, the activity of MnO should be lower than that of SiO_2 to satisfy the above condition. The compositional window corresponding to this condition is also shown as a circle in Fig. 7.

In summary, this experimental study of the slag-steel-inclusion multiphase equilibria for Si-Mn-killed steels found that the

MnO/SiO_2 ratio of the inclusions was relatively close to unity with varied Al_2O_3 content. From thermodynamic analyses of the steel-inclusion and the steel-slag systems, quantitative thermodynamic information for the slag-inclusion system was obtained. Finally, we propose the operating window of ladle slag in which the activity of MnO should be lower than that of SiO_2 for obtaining inclusions with a low melting point (< 1573 K) in Si-Mn-killed steel, which is treated in an alumina-lined ladle.

Conclusions

The thermodynamic equilibria between $CaO\text{-}Al_2O_3\text{-}SiO_2\text{-}CaF_2\text{-}MgO(\text{-}MnO)$ slag and Fe-1.5%Mn-0.5%Si-0.5%Cr melt was investigated at 1873 K in order to understand the effect of slag composition on the concentration of Al_2O_3 in the inclusions. Our major findings are as follows:

1. The activities of oxygen calculated from the $[Si]/(SiO_2)$ and $[Al]/(Al_2O_3)$ equilibria were in good agreement with those determined from classical Wagner formalism. The slag-metal reaction was believed to be in equilibrium in the present experiments.

2. The composition of the inclusions were mainly equal to $(MnO)/(SiO_2)=0.8(\pm0.06)$ (mol%) with Al_2O_3 content that was increased from about 10 to 40 mol% by increasing the basicity of the slag from about 0.7 to 2.1.

3. The $\log(X_{Al_2O_3} \cdot X_{MnO} / X_{SiO_2})$ of the inclusion was expressed as a linear function of the $\log[a_{Al}^2 \cdot a_{Mn} \cdot a_O^2 / a_{Si}]$ of the steel, indicating that the activity coefficient ratio of the inclusion components, $\gamma_{SiO_2}^i / (\gamma_{Al_2O_3}^i \cdot \gamma_{MnO}^i)$ was not significantly changed under the present experimental conditions.

4. The concentration of Al_2O_3 in the inclusions linearly increased with an increase in the activity ratio of slag components, $(a_{Al_2O_3}^s \cdot a_{MnO}^s / a_{SiO_2}^s)$, in a logarithmic scale. This linear relationship enabled determination of the appropriate compositional window of slag for obtaining inclusions with a low melting point in Si-Mn-killed steel refined in an alumina ladle.

References

1. R. Kiessling and N. Lange: *Nonmetallic Inclusions in Steels*, The Metals Society, London, 1978, Part. I.
2. A. Ghosh: *Secondary Steelmaking – Principles and Applications*, CRC press, Boca Raton, FL, 2001, pp. 255-69.
3. M.E. Fine: *Metall. Trans. A*, 1980, vol. 11A, pp. 365-79.
4. K. Kirihara: *Kobelco Technology Review*, 2011, no. 30, pp. 62-65.
5. S. Chen, M. Jiang, X. He and X. Wang: *Int. J. Min. Metall. Mater.*, 2012, vol. 19, pp. 490-98.
6. T. Fujisawa and H. Sakao: *Tetsu-to-Hagané*, 1977, vol. 63, pp. 1494-503.
7. T. Fujisawa and H. Sakao: *Tetsu-to-Hagané*, 1977, vol. 63, pp. 1504-11.
8. H. Suito and R. Inoue: *ISIJ Int*., 1996, vol. 36, pp. 528-36.
9. Y.B. Kang and H.G. Lee: *ISIJ Int*., 2004, vol. 44, pp.1006-15.
10. I.H. Jung, Y.B. Kang, S.A. Decterov and A.D. Pelton: *Metall. Mater. Trans. B*, 2004, vol. 35B, pp. 259-68.
11. C. Garlick, M. Griffiths, P. Whitehouse and C. Gore: *Ironmaking & Steelmaking*, 2002, vol. 29, pp. 140-46.
12. C. Bertrand, J. Molinero, S. Landa, R. Elvira, M. Wild, G. Barthold, P. Valentin and H. Schifferl: *Ironmaking & Steelmaking*, 2003, vol. 30, pp. 165-69.
13. S.K. Choudhary: *ISIJ Int*., 2011, vol. 51, pp. 557-65.
14. G. Okuyama, K. Yamaguchi, S. Takeuchi and K. Sorimachi: *ISIJ Int*. , 2000, vol. 40, pp. 121-28.
15. J.H. Park, D.S. Kim and S.B. Lee: *Metall. Mater. Trans. B*, 2005, vol . 36B, pp. 67-73.
16. J.H. Park and D.S. Kim: *Metall. Mater. Trans. B*, 2005, vol. 36B, pp. 495-502.
17. J.H. Park, S.B. Lee and H.R. Gaye: *Metall. Mater. Trans. B*, 2008, vol. 39B, pp. 853-61.
18. J.H. Park and H. Todoroki: *ISIJ Int*., 2010, vol. 50, pp. 1333-46.
19. J.H. Park, D.J. Kim, and D.J. Min: *Metall. Mater. Trans. A*, 2012, vol. 43A, pp. 2316-24.
20. J.S. Park, C. Lee, and J.H. Park: *Metall. Mater. Trans. B*, 2012, vol. 43B, pp. 1550-64.
21. *Thermodynamic Data for Steelmaking*, ed. by M. Hino and K. Ito, The Japan Society for the Promotion of Science, The 19th Committee on Steelmaking, Tohoku University Press, Sendai, 2010.
22. F. Ishii and S. Ban-ya: *ISIJ Int*., 1992, vol. 32, pp. 1091-96.
23. K. Suzuki, S. Ban-ya and M. Hino: *ISIJ Int*., 2001, vol. 41, pp. 813-17.
24. T. Itoh, T. Nagasaka and M. Hino: *ISIJ Int*., 2000, vol. 40, pp. 1051-58.
25. K. Takahashi and M. Hino: *High Temp. Mater. Proc*., 2000, vol. 19, pp. 1-10.
26. H. Itoh, M. Hino and S. Ban-ya: *Tetsu-to-Hagané*, 1997, vol. 83, pp. 773-78.
27. H.R. Gaye: *in The Making, Shaping and Treating of Steel*, 11th ed., Casting Volume, The AISE Steel Foundation, Pittsburgh, PA, 2003.
28. Z. Hong, X. Wu and C. Kun: *Steel Res.*, 1995, vol. 66, pp. 72-76.
29. www.factsage.com.
30. C.W. Bale, E. Belisle, P. Chartrand, S.A. Decterov, G. Eriksson, K. Hack, I.H. Jung, Y.B. Kang, J. Melancon, A.D. Pelton, C. Robelin and S. Petersen: *Calphad*, 2009, vol. 33, pp. 295-311.
31. M.O. Suk and J.H. Park: *J. Am. Ceram. Soc*., 2009, vol. 92, pp. 717-23.
32. J.H. Park, I.H. Jung and S.B. Lee: *Met. Mater. Int*., 2009, vol. 15, pp. 677-81.
33. J.H. Park: *Met. Mater. Int*., 2010, vol. 16, pp. 987-92.
34. J.H. Park, J.G. Park, D.J. Min, Y.E. Lee and Y.B. Kang: *J. Eur. Ceram. Soc*., 2010, vol. 30, pp. 3181-86.
35. J.H. Park, M.O. Suk, I.H. Jung, M. Guo and B. Blanpain: *Steel Res. Int*., 2010, vol. 81, pp. 860-68.
36. J.H. Park, G.H. Park and Y.E. Lee: *ISIJ Int*., 2010, vol. 50, pp. 1078-83.
37. G.H. Park, Y.B. Kang and J.H. Park: *ISIJ Int*., 2011, vol. 51, pp. 1375-82.
38. Y.B. Kang and J.H. Park: *Metall. Mater. Trans. B*, 2011, vol. 42B, pp. 1211-17.
39. K.Y. Ko and J.H. Park: *Metall. Mater. Trans. B*, 2011, vol. 42B, pp. 1224-30.
40. J.H. Park and G.H. Park: *ISIJ Int*., 2012, vol. 52, pp. 764-69.
41. K.Y. Ko and J.H. Park: *Metall. Mater. Trans. B*, 2012, vol. 43B, pp. 440-42.
42. D.J. Kim and J.H. Park: *Metall. Mater. Trans. B*, 2012, vol. 43B, pp. 875-86.
43. J.H. Park: *ISIJ Int*., 2012, vol. 52, pp. 1627-36.
44. J.H. Heo, S.S. Park and J.H. Park: *Metall. Mater. Trans. B*, 2012, vol. 43B, pp. 1098-105.
45. J.H. Park: *ISIJ Int*., 2012, vol. 52, pp. 2303-04.
46. J.H. Park: *Met. Mater. Int*., 2013, vol. 19, pp. 577-84.
47. J.H. Park: *Steel Res. Int*., 2013, vol. 84, accepted, in print. DOI: 10.1002/srin.201200210.
48. K. Tomioka, K. Ogawa and H. Matsumoto: *ISIJ Int*., 1996, vol. 36, pp. S101-04.